A new assessment in North Atlantic waters of the relationship between DMS concentration and the upper mixed layer solar radiation dose

Sauveur Belviso, Guy Caniaux

A new assessment in North Atlantic waters of the relationship between DMS concentration and the upper mixed layer solar radiation dose

S. Belviso[1] and G. Caniaux[2]

Received 16 September 2008; revised 6 January 2009; accepted 12 January 2009; published 18 March 2009.

[1] The results of the POMME experiment, conducted in the northeast Atlantic Ocean in 2001, were used to explore whether dimethylsulfide (DMS) concentrations are linked to epipelagic ecosystem exposure to solar radiation as proposed by Vallina and Simó (2007). According to the seasonal variations in the DMS-to-dimethylsulfoniopropionate (DMSP) ratio, we found that the summer surface water concentration of DMS was, on average, threefold higher than expected from the abundance of DMSP. This is in agreement with previous observations and confirms that seasonal changes in the trophic regime, from mesotrophy in winter and spring to oligotrophy in summer, are accompanied by a relative enhancement of DMS over DMSP. However, contrary to the observations carried out at Hydrostation S in the northwest Atlantic Ocean, no strong relationship between DMS and the solar radiation dose (SRD) exists in the northeast Atlantic Ocean. From a series of sensitivity tests, where different combinations of the three parameters that drive the SRD were investigated (i.e., the solar irradiance, the law of its attenuation in the sea, and the mixed layer depth), we found that the SRD accounted for only 19% to 24% of the variance associated with monthly surface DMS concentrations. Additionally, the slope of the relationship between DMS and SRD was particularly sensitive to the choice of the irradiance attenuation law. Overall, we find that the DMS versus SRD relationship is much less significant in the northeast Atlantic Ocean than in the Sargasso Sea. In addition, we suggest a large impact of algal community structure on summer DMS concentrations in the mesotrophic coastal waters of the Mediterranean Sea. Therefore, we question the consistency between DMS versus SRD relationships at local, basin, and global scales and propose that empirical relationships relating DMS to SRD be applied with caution.

Citation: Belviso, S., and G. Caniaux (2009), A new assessment in North Atlantic waters of the relationship between DMS concentration and the upper mixed layer solar radiation dose, *Global Biogeochem. Cycles*, *23*, GB1014, doi:10.1029/2008GB003382.

1. Introduction

[2] Although dimethylsulfoniopropionate (DMSP) is the major precursor of dimethylsulfide (DMS), there is compelling evidence that surface water concentrations of DMS can be substantially higher than expected from the abundance of DMSP. Indeed, large spatial and temporal variations in the sea surface DMS-to-DMSP ratio have been frequently observed, either along tracks of research vessels [*Andreae*, 1990; *Belviso et al.*, 2000a, 2003] or at monitoring sites [*Dacey et al.*, 1998; *Vila-Costa et al.*, 2008]. The underlying reason for the relatively high abundances of DMS was initially attributed to shifts in trophic regimes, since the DMS-to-DMSP ratio in oligotrophic waters was substantially higher than in mesotrophic or eutrophic systems [*Andreae*, 1990; *Aumont et al.*, 2002; *Belviso et al.*, 2003, 2004a]. However, it is unlikely that a shift from mesotrophy to oligotrophy explains the increasing trend in the DMS-to-DMSP ratio observed at Hydrostation S in the Sargasso Sea between springtime and late summer, since oligotrophic conditions are already well established in the springtime [*Dacey et al.*, 1998].

[3] Although the seasonality in DMS is certainly determined by the interplay between several physical and biogeochemical processes [*Archer*, 2007], *Vallina and Simó* [2007] (hereinafter referred to as VS07), suggested that the upper mixed layer solar radiation dose (SRD) was the driving factor behind the relative accumulation of DMS in oligotrophic and mesotrophic waters during summer. VS07 provided data from two time series in the Sargasso Sea (at Hydrostation S) and in the coastal Mediterranean Sea (at the Bay of Blanes monitoring station) to support their assertion. However, the relationship between DMS and SRD for the Bay of Blanes requires a more detailed consideration for two reasons:

[1] Laboratoire des Sciences du Climat et de l'Environnement, UMR1572, IPSL, CEA, UVSQ, CNRS, Gif-sur-Yvette, France.
[2] Centre National de Recherches Météorologiques, GAME, Météo-France, CNRS, Toulouse, France.

0886-6236/09/2008GB003382

Table 1. Criteria Used to Determine the Mixed Layer Depth[a]

Criteria	MLD Threshold Criteria	Zref (m)
A	$\Delta T = 0.2°C$	0
B	$\Delta T = 0.1°C$	5
C	$\Delta\sigma_\theta = 0.01$ kg/m^3	5
D	$\Delta\sigma_\theta = 0.02$ kg/m^3	5
E	$\Delta(\delta\sigma_\theta/\delta z) = 0.002$ kg/m^4	5
F	$\Delta\sigma_\theta = \sigma_\theta(T+\Delta T,S) - \sigma_\theta(T,S)$ with $\Delta T = 0.1°C$[b]	5
G	Norm error = 0.1[c]	5

[a]The mixed layer depth (MLD) is the depth at which the temperature **T** or potential density σ_θ change by a given threshold relative to the temperature or potential density depth Zref.
[b]*Kara et al.* [2000].
[c]*Thomson and Fine* [2003].

[4] First, data selection removed the May–June 2004 data points [see *Vila-Costa et al.*, 2008, Figure 2b] to construct Figure 1 in VS07. Consequently, DMS levels associated with SRDs between 250 and 300 W m^{-2} did not range between 7 and 9 nM but, in fact, between 7 and 20 nM, a considerably larger degree of variability. The exclusion of those high DMS concentrations was likely for consistency with data treatment used for the investigation of the DMS versus SRD relationship at the global scale (VS07, Figure 4). Indeed, a cut-off criterion, roughly corresponding to an upper limit of 10 nM, was applied specifically to exclude high DMS values associated with eutrophic coastal systems and local blooms of algae that produce very high amounts of DMSP. The DMSP concentrations in the Bay of Blanes, however, were far from being typical of eutrophic coastal systems and the DMSP levels recorded in summer 2004 in the Bay of Blanes were only slightly higher than those for the summer 2003 [*Vila-Costa et al.*, 2008]. So it appears that the exclusion of these two data points, which strongly impacted the coefficient and slope of the DMS versus SRD regression line, was likely not appropriate for coastal Mediterranean waters.

[5] Second, a series of observations suggest that the summer high DMS levels in the Bay of Blanes might result from changes in SRD, but likely also arise from changes in algal communities. Indeed, dinoflagellates, including the photosynthetic dinoflagellate *Gymnodinium impudicum* (= *Gyrodinium impudicum*), proliferate in Blanes harbor and in the bay during summer [*Vila and Masó*, 2005; *Vila-Costa et al.*, 2008]. Moreover, *G. impudicum* is an important DMSP producer and a diel vertical migrant who spends the light hours at the sea surface [*Belviso et al.*, 2000b]. It is also known that even a relatively low concentration of photosynthetic dinoflagellates would contribute significantly to both DMSP lyase activity and DMSP production [*Steinke et al.*, 2002]. However, it is likely that the contribution of dinoflagellates to early summer DMS production in the coastal Mediterranean Sea was lower than in the North Atlantic. Accordingly, while in June 2003 the maximum contribution of DMSP producers in the greater than 5 μm size fraction was about 18% in the Bay of Blanes [*Vila-Costa et al.*, 2008], about 50% of the particulate DMSP in North Atlantic surface waters was found in the greater than 10 μm size fraction [*Steinke et al.*, 2002].

[6] Hence, there is a need for new seasonal time series to provide the necessary support for a strong relationship between DMS and the upper mixed layer solar radiation dose at the regional scale. In this study we aim to conduct a new evaluation of the DMS versus SRD relationship in North Atlantic waters. The study area was located in the northeast Atlantic (16–22°W, 38–45°N) about 10° of latitude north of the latitude of Hydrostation S, far away from the coast. Data were collected during the three cruises of the Programme Océan Multidisciplinaire Méso-Echelle (POMME) experiment which took place in 2001 in the northeast Atlantic [*Mémery et al.*, 2005]. The experimental strategy included three hydrological surveys conducted during specific periods: POMME1 (P1) which took place from 3 to 23 February, so at the onset of the spring bloom, estimated the maximum winter mixed layer depths and described the initial prebloom conditions; POMME2 (P2), from 24 March to 12 April, had the objective of characterizing the spring bloom; finally POMME3 (P3), from 23 August to 13 September, was conducted during the late summer oligotrophic regime. During P1 and P2, special care was taken to document the air-sea fluxes and their relationship with near surface water properties [*Caniaux et al.*, 2005a; *Giordani et al.*, 2005]. Some of these data (conductivity-temperature-depth (CTD), solar radiation fluxes, mixed layer depths) are used in this paper.

2. Methods

[7] As proposed by VS07, a measure of the underwater irradiance available for buoyant particles and dissolved substances can be computed from the Solar Radiation Dose (SRD) which is defined as the integral of the available irradiance at all depths within the mixed layer. The relationship established by VS07 between the SRD and DMS depends largely [*Toole and Siegel*, 2004] on the mixed layer depth (MLD) and the underwater irradiance attenuation law [*Paulson and Simpson*, 1977; *Simpson and Dickey*, 1981]. In the following analysis, close attention is paid to the uncertainties associated with each parameter and formula choice when calculating the SRD.

2.1. Mixed Layer Depth

[8] Combined with the Sea Surface Temperature (SST) and the Sea Surface Salinity (SSS), the MLD is a good diagnostic for the upper layer stratification. However, the concept of MLD is arbitrary [*de Boyer Montégut et al.*, 2004]. Its definition depends on the choice of (1) a computation method (e.g., the threshold method [*Kara et al.*, 2000] and the segment method [*Thomson and Fine*, 2003]), (2) a threshold criterion (on the temperature, the density, the density gradient, or else on the error norm value of the linear fit to the data in Thomson and Fine's method), and (3) a reference depth (or initial search level) to avoid problems associated with the diurnal evolution in the top layers. As the choice of the MLD definition and of the criterion adopted for its calculation impacts the computation of the SRD, several sensitivity tests were carried out. Seven criteria are tested (Table 1): two using temperature thresholds ("A" is like in VS07 for their Blanes Bay case and "B" for their Bermuda and global ocean cases), three using potential density thresholds ("C," "D," and "F"), "E" uses a criterion on the vertical gradient of the potential density and "G" is the *Thomson and Fine* [2003] method.

2.2. Choice of the Incoming Solar Irradiance

[9] Incoming Solar Radiance (ISI) was recorded on board the R/V *l'Atalante*, the ship used to cover the network of hydrological stations during P1 and P2. Since no ISI was measured on board the ship during P3, only satellite products are used for the summer period. As will be shown later, in situ and satellite records display high consistency in the POMME area.

[10] ISI data of high quality were acquired in situ every 10 s and then averaged every 10 min [*Caniaux et al.*, 2005a]. It allows for the calculation of the ISI several hours before the CTD cast (typically 24 h) as a measure of the available energy received by the phytoplankton. However, there are some limitations to the use of the in situ ISI data. The duration of each hydrographic station was about 3 h and the ship then steamed to the next station a distance of fifty kilometers. So, no fixed measurements of ISI of long enough duration are available at each CTD location. Moreover, because of the highly time and space varying cloud cover, the incoming solar irradiance cannot be considered as synoptic. It is the reason why in situ and satellite ISI data were crosschecked during the winter and spring cruises.

[11] Satellite ISI retrievals were largely used for modeling purpose during POMME [e.g., *Paci et al.*, 2005, 2007]. These data were produced operationally by the Centre de Météorologie Spatiale of Météo-France (Lannion, France) from METEOSAT data with the method described by *Brisson et al.* [1994]. Gridded, daily fields were reconstructed on a regular, 10 km horizontal grid (original data were acquired at a resolution of 0.04° of longitude and latitude and at a temporal resolution of 1 h). These data are thus available at the exact position of each CTD and are used to calculate the irradiance reaching the water column some days before the CTD cast. Note that comparisons between satellite, ship data and extra buoy data were performed by *Caniaux et al.* [2005a] and the statistics obtained (bias lower than 3W/m^2, correlation r = 0.98) proved that satellite irradiances are good enough to extend the confidence in satellite-derived fluxes at the mesoscale to all seasons in the northeast Atlantic.

2.3. Choice of the SRD Formula

[12] In the upper water column, each wavelength of light attenuates, following an exponential decay function of the Beer-Lambert type. The vertical distribution of downward irradiance in the water column can thus be obtained as the integral over the whole spectrum of the solar irradiance per unit wavelength multiplied by its exponential attenuation function. Classically, this vertical distribution has been approximated by a one exponential parameterization:

$$I(z) = I_0 \exp(-z/D)$$

where I_0 is the incident less reflected and emergent irradiance at the surface and D the attenuation length, assumed to be constant with depth; here I(z) stands for the downward irradiance at depth z. If this parameterization is a good approximation of absorption for the blue-green light under a depth of 10m, several authors have noted that the approximation is less good above 10m because of the preferential absorption of the short- and long-wave components of light. As proposed by *Paulson and Simpson* [1977], the bimodal exponential parameterization:

$$I(z) = I_0\{R.\exp(-z/D1) + (1-R).\exp(-z/D2)\}$$

is a simple parameterization that better represents the attenuation of light. This formula introduces a partitioning constant R between the red spectral component (first term in the right hand side of the equation with a constant extinction depth D1) and the blue-green one (second term with extinction depth D2). Although several other complicated schemes for adjusting the underwater irradiance exist, for instance using many wavelength bands [*Paulson and Simpson*, 1981], this bulk parameterization seems to provide fairly good performance for modeling the light attenuation and most biological and chemical processes inside the mixed layer [*Simpson and Dickey*, 1981]. The choice of R, D1 and D2 depends on the mean optical properties of the water type and are assigned using *Jerlov*'s [1977] water type classification. These parameters have been statistically adjusted for the domain and time period of the POMME experiment by *Caniaux et al.* [2005b] resulting in R = 0.74, D1 = 1.3m and D2 = 20m as reference values. Finally, two definitions of the SRD are used in this study:

$$SRD1 = \frac{1}{MLD}\int_0^{MLD} I_0 \exp(-z/D)dz$$

$$SRD2 = \frac{1}{MLD}\int_0^{MLD} I_0\{R.\exp(-z/D1) + (1-R).\exp(-z/D2)\}dz$$

That is, after integration:

$$SRD1 = \frac{I_0 D}{MLD}\{1 - \exp(-MLD/D)\}$$

$$SRD2 = \frac{I_0}{MLD}\{R.D1(1-\exp(-MLD/D1)) + (1-R).D2(1-\exp(-MLD/D2))\}$$

[13] SRD1 is the same formula as in VS07 with an extinction light coefficient (inverse of the extinction depth) of 0.06m^{-1}. In the rest of the paper, SRD2 is referred to as *Paulson and Simpson* [1977]'s formula using the R, D1 and D2 adjusted for POMME as mentioned previously.

2.4. Analysis of Sensitivity Tests Using Taylor Diagrams

[14] The *Taylor* [2001] diagram is an easy and concise way of presenting statistical results concerning an ensemble of sensitivity tests. It simultaneously compares several frequently used statistics: the standard deviation, the correlation coefficient, and the pattern root mean square (RMS) error. This diagram will be used for analyzing the results of this study and is briefly presented in this section. A

reference series is defined (denoted *Rf*) and each test series (denoted *Te*) can provide a correlation coefficient *r*:

$$r = \frac{\frac{1}{N}\sum_{n=1}^{N}(Rf(n)-\overline{Rf})(Te(n)-\overline{Te})}{\sigma_{Rf}\sigma_{Te}}$$

where N is the number of CTD used, $\overline{Rf}$ and $\overline{Te}$ are the mean values of the reference and test series respectively, and σ_{Rf} and σ_{Te} their respective standard deviations.

[15] A centered RMS difference *e* between two series can also be defined:

$$e = \left\{\frac{1}{N}\sum_{n=1}^{N}\left[(Rf(n)-\overline{Rf})-(Te(n)-\overline{Te})\right]^2\right\}^{1/2}$$

and, finally, a skill score, *s* [*Taylor*, 2001]:

$$s = \frac{4(1+r)}{\left(\frac{\sigma_{Rf}}{\sigma_{Te}}+\frac{\sigma_{Te}}{\sigma_{Rf}}\right)^2(1+r_0)}$$

where r_0 is the maximum correlation attainable between the ensemble of test series. The skill score *s* varies from 0 (the limit when the correlation is lowest and the standard deviation of the test series approaches 0 or infinity; least skillful) to 1 (the limit reached when the correlation is maximum and the test standard deviation approaches that of the reference series; most skillful). Moreover, the skill score decreases when the test variance increases; for small test variances the skill is proportional to the variance and for large variances, the skill is inversely proportional to the variance.

[16] In the *Taylor* [2001] diagram, the points are plotted on a polar graph: the radial distance from the origin is proportional to the standard deviation of the series and its azimuthal position is the correlation coefficient with the reference series. Naturally, the reference series is plotted along the horizontal axis. This diagram thus quantifies the degree of similarity of any test series with the reference. Isolines of the skill score drawn on the diagram allow characterization of the test series placing more emphasis on the reference variance.

2.5. DMS(P) Analysis

[17] Vertical profiles of DMS and total DMSP (DMSPt) were carried out in the upper 80 m of the water column and analyses were performed at sea following the methodology described by *Belviso et al.* [2003]. Discrete water samples were taken from Niskin bottles mounted on a CTD carrousel. The network of hydrographic stations from which DMS and DMSPt contour plots were constructed is shown by *Belviso et al.* [2004a]. DMS measurements taken at a single depth in the upper mixed layer (5 ± 3m) are used in the following, as per VS07.

2.6. Enumeration of Suspended Particles

[18] Suspended particles in the range 1.5–100 μm were routinely counted and sized using an optical HIAC counter (Royco-Pacific Scientific). Discrete water samples were taken for subsequent enumeration of particles and DMS(P) analysis from the same Niskin bottles. More details on the HIAC measurements can be found in the work of *Belviso et al.* [2003]. In the latter, as in the present study, the enumeration of suspended particles was of higher utility as a surrogate for DMSPt than chlorophyll *a* (data not shown). Here, the enumeration of suspended particles is used as a descriptor of all microbial populations (size > 1.5 μm) to ascertain that the DMS variations do not result from changes in plankton communities not resolved at the organismic level.

3. Results

3.1. MLD: Spatiotemporal Variations and Sensitivity

[19] Individual CTD profiles from the three hydrological networks of POMME (78 during P1, 80 during P2 and 74 during P3, i.e., a total of 232 CTD profiles) are used to construct the series of MLD plotted in Figure 1a. For reasons of clarity, the results of four among the seven sensitivity tests are shown in Figure 1a. In winter (P1), when the stratification is weak, MLDs are the deepest (they range from 10m to 275m) but are very sensitive to the choice of the criterion adopted since MLD can vary by up to 150m depending on the criterion. Conversely, in summer (P3), when the stratification at the MLD base is stronger, this choice is less crucial. The criterion "A" (depending on the SST) tends to overestimate MLDs in spring (P2) and the criterion "E" (vertical gradient of potential density) overestimates the deepest MLDs and frequently underestimates the summer (P3) MLDs. *Thomson and Fine* [2003] criterion ("G," data not shown) also underestimates summer MLDs because it is very sensitive to small heterogeneities in the density profiles. We also found that the diurnal evolution of the mixed layer could be important even in winter (e.g., under anticyclonic weather regime with weak wind and strong solar irradiance). This resulted in a temporary diurnal stratification with important MLD fluctuations between day and night, which implies that the reference depth is an important parameter, the latter leading to the observed differences between criteria "C" and "D," specially during P1 and P2 (data not shown). In agreement with *Caniaux et*

Figure 1. Time series of (a) mixed layer depth (m) computed from different criteria applied to conductivity-temperature-depth data collected during cruises P1 (winter, 2001), P2 (spring), and P3 (summer): criteria "A," "B," "D,"and "E" are defined in Table 1; (b) satellite and ship solar irradiances (W/m^2); (c) mixed layer depth (MLD) solar radiation dose: criteria "A," "E," "G,"and "K" are adapted to the winter and spring situations whereas criteria "B," "F," "H,"and "L" are for the summer one, both sets of criteria being defined in Table 2; (d) sea surface DMS(Pt) concentrations and DMS-to-DMSPt ratios. The parameters are plotted against station number, not against time, because the time series were not performed always at the same sampling site but on a grid of 5.5° × 4° grid size.

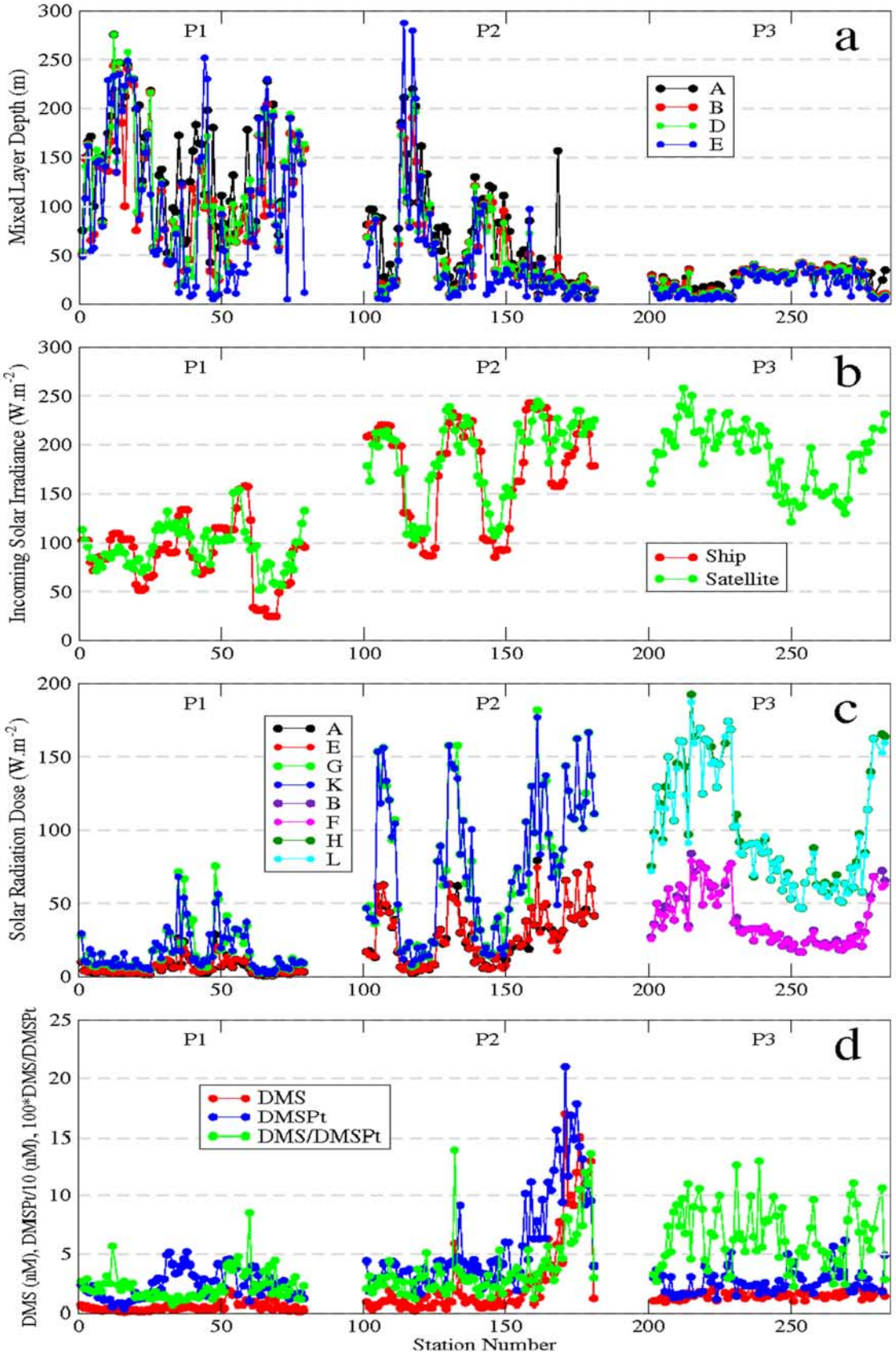
a
P1
P2
P3
Mixed Layer Depth (m)
A
B
D
E
b
Incoming Solar Irradiance (W.m-2)
Ship
Satellite
c
Solar Radiation Dose (W.m-2)
A
E
G
K
B
F
H
L
d
DMS (nM), DMSPt/10 (nM), 100*DMS/DMSPt
DMS
DMSPt
DMS/DMSPt
Station Number

Figure 1

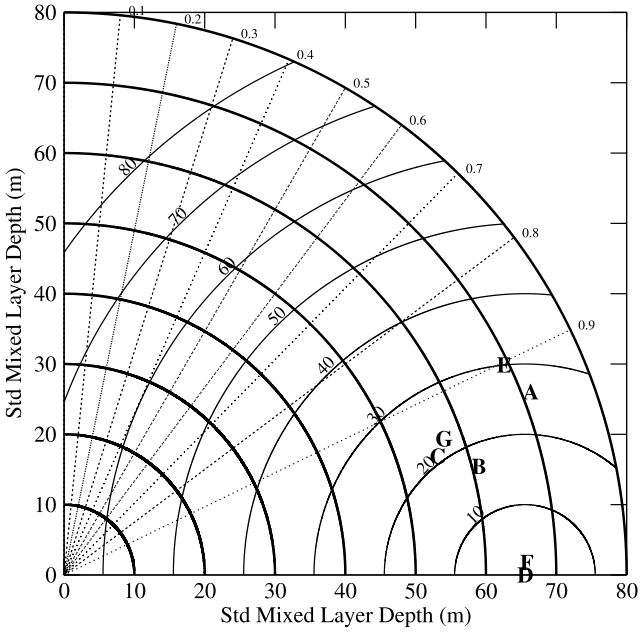

Figure 2. *Taylor* [2001] diagram applied to the MLD computed from seven options defined in Table 1. Black circles in bold which are centered on the origin refer to the standard deviation of the test series (labeled D). Black isolines centered on the reference series D refer to the centered root mean square (RMS) difference between the test and reference series. Dotted lines refer to the correlation between the test and reference series.

al. [2005b], the most appropriate criterion, valid for both strongly to weakly stratified hydrographic data, over the whole duration of the POMME experiment, seems to be the criterion "D" (density threshold of 0.02 kg/m^3 with a reference depth of 5 m); this criterion will be our best estimate used in the rest of this study. In terms of correlation and standard deviation of the MLD series, the criterion "F" [*Kara et al.*, 2000] appears closest to the reference, and rather close to criterion "B," i.e., that applied to Hydrostation S's CTD data in VS07, and to criteria "C" and "G" (Figure 2). Conversely, criterion "A," i.e., that applied to Blanes Bay's CTD data in VS07, and criterion "E," are the farthest.

3.2. ISI: Spatiotemporal Variations

[20] Figure 1b compares the ship (exactly 24 h before the CTD) and satellite derived (half the ISI sum from the day of the CTD and the day before) ISI at each CTD station during P1 and P2. Daily ISI values range between 25 and 160 W/m^2, 80 and 250 W/m^2, and 125 and 260 W/m^2, during P1, P2 and P3, respectively. Differences arise from the fact that (1) ship data were recorded along the trajectory, but satellite at the exact location of the CTD, (2) the coverage period does not exactly coincides between the two data sets, and (3) some difference exists between in situ and satellite retrievals. Nonetheless, the linear regression between both data sets was

$$\text{Satellite ISI} = 0.82 \times \text{ship ISI} + 33.3$$

(r^2 = 0.80; n = 158; mean error estimate: 25.4 W/m^2; the two series have a mean bias of 9.5 W/m^2 and root mean square error of 29.3 W/m^2). These statistics can thus be considered as satisfactory. For both the ship series and satellite retrievals, a constant albedo of 0.06 was assumed and applied to the downward I_0 solar radiation for calculating the SRD.

3.3. SRD: Spatiotemporal Variations and Sensitivity

[21] In this section, the SRD has been computed from the different options of MLD, ISI and solar irradiance attenuation law (SRD1, SRD2). However, the number of MLD criteria has been reduced (3 remained over 7, i.e., criteria "A," "B" and "D" listed in Table 1; MLD criteria "A" and "B" were adopted because used by VS07, and MLD criterion "D" is used as a reference) in order to limit the number of sensitivity tests which were reduced to a total number of 12. These criteria are detailed and listed in Table 2. According to SRD criterion "A" (Table 2), values were lower during P1 (winter), less than 30 W/m^2, and increased on average during P2 (spring) and P3 (summer) because of increased solar radiation and shallower MLDs (Figure 1c). However, large day-to-day fluctuations were recorded during P2, with large variations due to the method of calculation, particularly during P2 and P3 during which SRD values can more than double (up to 100 W/m^2 when using SRD2 and 200 W/m^2 when using SRD1). Accordingly, we performed sensitivity tests prior to evaluating any relationship between SRD and DMS.

[22] The sensitivity tests are presented in Figure 3 using *Taylor* [2001] diagrams. The reference SRD series for cruises P1 and P2 (i.e., "A" in Table 2 and Figure 3a) is defined by using: (1) the criterion "D" for the MLD as previously mentioned, (2) ship ISI because of the high quality of the data set, and (3) *Paulson and Simpson*'s [1977] formula (SRD2). Since only satellite data is available for P3, so the reference SRD series for that cruise is "B" (Table 2 and Figure 3b).

[23] Estimates of SRD are most sensitive to the irradiance attenuation law whatever the periods considered (winter and spring (Figure 3a) and summer (Figure 3b)). Indeed, the plots clearly indicate the existence of two distinct groups of points: one group assigned with the SRD1 formula (implying much larger standard deviation and much less skillful,

Table 2. Criteria Used to Determine the Surface Radiation Dose

Criteria	SRD Formula	MLD Threshold Criteria	Zref (m)	ISI Data
A	SRD2	$\Delta\sigma_\theta$ = 0.02 kg/m^3	5	Ship
B	SRD2	$\Delta\sigma_\theta$ = 0.02 kg/m^3	5	Satellite
C	SRD2	ΔT = 0.2°C	0	Ship
D	SRD2	ΔT = 0.2°C	0	Satellite
E	SRD2	ΔT = 0.1°C	5	Ship
F	SRD2	ΔT = 0.1°C	5	Satellite
G	SRD1	$\Delta\sigma_\theta$ = 0.02 kg/m^3	5	Ship
H	SRD1	$\Delta\sigma_\theta$ = 0.02 kg/m^3	5	Satellite
I	SRD1	ΔT = 0.2°C	0	Ship
J	SRD1	ΔT = 0.2°C	0	Satellite
K	SRD1	ΔT = 0.1°C	5	Ship
L	SRD1	ΔT = 0.1°C	5	Satellite

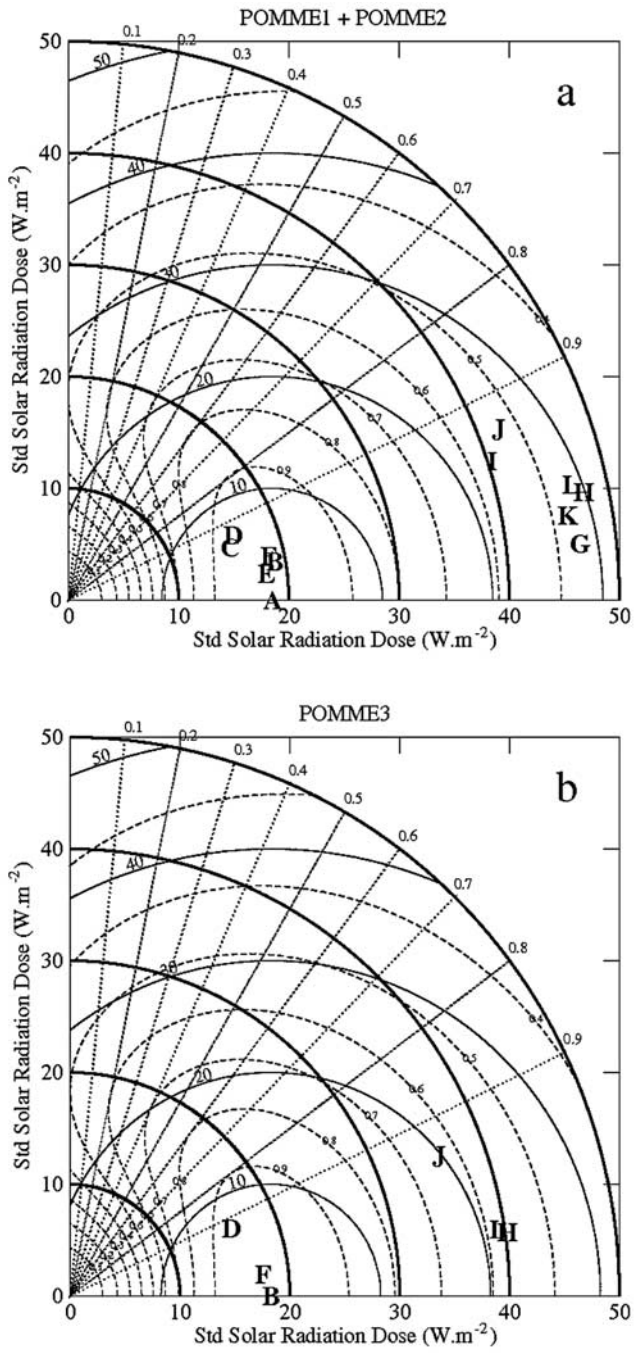

Figure 3. *Taylor* [2001] diagrams applied to the SRD computed from 12 options (Table 2); (a) from P1 and P2 data sets; and (b) from P3 data set. Black circles in bold which are centered on the origin refer to the standard deviation of the test series; black isolines centered on the reference series (criterion "A" for P1 and P2, criterion "B" for P3, both located on the horizontal axis) refer to the centered RMS difference between the test and reference series. Dashed isolines refer to the measure of the skill (see section 2.4), and the radial black dotted lines refer to the correlation between the test and reference series.

relative to the reference) and the other with SRD2 (comparable standard deviation and more skillful, relative to the reference series). They indicate that the SRD is most sensitive to the choice of the parameterization of the penetration of solar irradiance, with SRD values frequently twice higher with SRD1, compared to SRD2 during P2 or P3 (Figure 1c). We note that similar results were obtained when using an extinction light coefficient of $0.07m^{-1}$ (not shown) in SRD1 instead of $0.06m^{-1}$. Also apparent is that the choice of the MLD criterion is less critical than the law of solar radiation penetration: this is due to the rapid attenuation of the light in the upper first meters that are well inside the mixed layer (whatever the criterion used to define its depth). Finally, in our case, choosing ship or satellite solar irradiance data has low sensitivity on the SRD, because of the small differences between the two data sets (Figure 1b).

3.4. Mesoscale Variability of DMSP and DMS Concentrations

[24] Overall, we find a large degree of decoupling between DMSPt and DMS concentrations. The spatiotemporal variations of the DMS(Pt) concentrations and of the DMS-to-DMSPt ratio at the sea surface are shown in Figure 1d. Only three DMS "hot spots" were observed, once during the second half of cruise P1 when it reached about 2 nM, and twice during P2 (up to about 6 nM and 17 nM, respectively). A significant increase in the DMS-to-DMSPt ratio occurred between winter and spring, but the major one was observed between spring and summer. Indeed, the median value of the ratio (to minimize the influence of the large degree of variance) was equal to 0.02 in winter, whereas it was 50% and threefold higher in spring and summer, respectively.

[25] Contour plots of sea surface DMSPt and DMS concentrations were assembled from about 70–80 vertical profiles carried out during each cruise (Figure 4). During winter, the spatial distribution of DMSPt was strongly influenced by stratification since its concentration was enhanced (30–50 nM) in areas with mixed layer depths (defined using criterion "D," Table 1) shallower than 90 m (Figure 4a). Surprisingly, the DMS and DMSPt spatial distributions did not coincide, since the richest area in DMS was restricted to the southwestern sector of the stratified zone (Figure 4d). In fact, DMS peaked (1.2–2 nM) at the location of an anticyclonic eddy labeled A2 [*Le Cann et al.*, 2005]. As a consequence, the DMS-to-DMSPt ratio was not homogeneously distributed within the stratified zone but was maximal in the sector of A2 (0.04–0.08, data not shown). During spring, huge increases in DMSPt and DMS levels were observed and both spatial distributions are more coherent than during winter (Figures 4b and 4e). Both compounds exhibited more pronounced peaks in the southwestern sector of the POMME area (DMSPt: 120–180 nM, DMS: 10–16 nM), a highly stratified zone with mixed layer depths shallower than 20–30m, coinciding with the location of the anticyclonic eddy A2. There, the DMS-to-DMSPt ratio was in the range 0.07–0.13 (data not shown), about twice the winter values. Note that the stratified areas to the north and to the northeast displayed

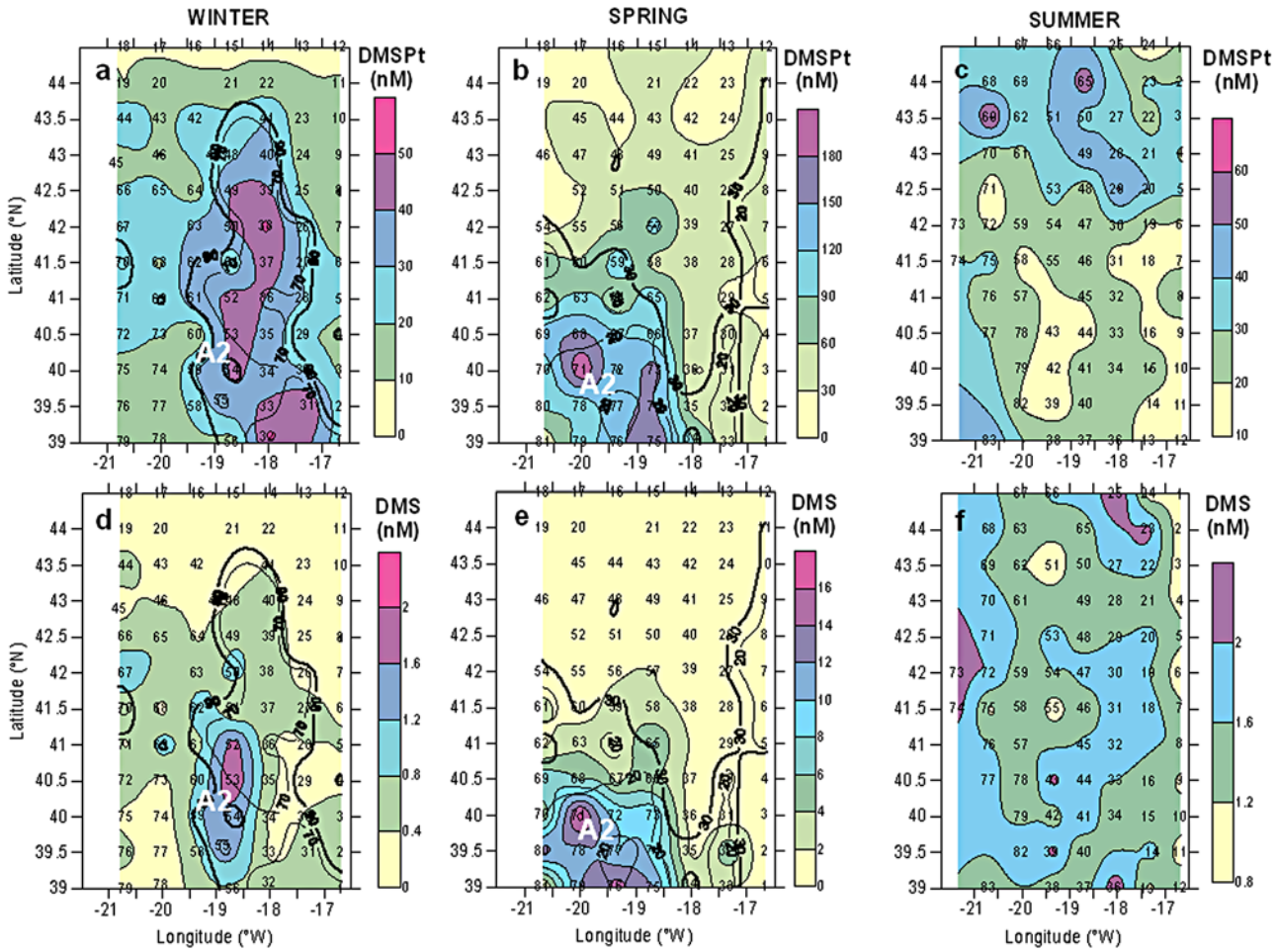

Figure 4. Spatial distribution of sea surface DMSPt and DMS concentrations at the three seasons investigated over the POMME area. Selected mixed layer depth contours are superimposed to document the impact of stratification on the distribution of sulfur compounds (90 and 70 m and 20 and 30 m isocontours in winter and spring, respectively). Grid numbers indicate station positions and reference numbers. A2 is an anticyclonic eddy tracked from September 2000 to August 2001. It displayed a consistent southwestward translation [*Le Cann et al.*, 2005].

considerably lower levels of DMSPt and DMS (10–60 nM, 0.5–2 nM, respectively), and lower DMS-to-DMSPt ratios (0.01–0.04). During summer, although the POMME area was rather homogeneously stratified (MLDs were in the range 15–35 m), a clear zonation in DMSPt was observed, concentrations in the area north of 42–42.5°N (30–60 nM, Figure 4c) being substantially higher than south of this line (10–30 nM). However, the DMS distribution did not mimic that of DMSPt (Figure 4f). Hence, the DMS-to-DMSPt ratio exhibited a north-south gradient with highest values in the southern part of the POMME area (data not shown).

[26] Figures 5a and 5c demonstrate the utility of the enumeration of suspended particles as a surrogate for total DMSP, but not DMS, in the POMME area (Figure 5a) and at a larger scale (Figure 5c). Indeed, a different sector of northeastern Atlantic Ocean was surveyed during the PROSOPE cruise (Cape Ghir (Morocco) to Gibraltar). This survey extended also in the Mediterranean Sea, from Gibraltar to the Ionian Sea [*Belviso et al.*, 2003]. It is worthy to note that the POMME and PROSOPE data sets exhibited comparable ranges in DMSP and particle concentrations. The linear regressions between DMSPt concentration and the number of suspended particles (r^2 = 0.66 and r^2 = 0.77, Figures 5a and 5c, respectively), calculated with log-transformed data, are stronger than those between concentrations of particles and DMS (r^2 = 0.21 and r^2 = 0.10, Figures 5b and 5d, respectively). Hence, the concentration of DMS in oligotrophic surface waters (in the Ionian Sea and during P3) is markedly higher than expected on the abundance of suspended particles whereas no such contrast is observed for total DMSP.

3.5. DMS Versus SRD and Sensitivity Tests

[27] No strong statistical relationship between DMS and SRD could be deduced from the POMME data set, regardless of the season considered. In the scatter plot assembled from sea surface DMS concentrations and SRDs (Figure 6), data from individual cruises are distinguished but the linear

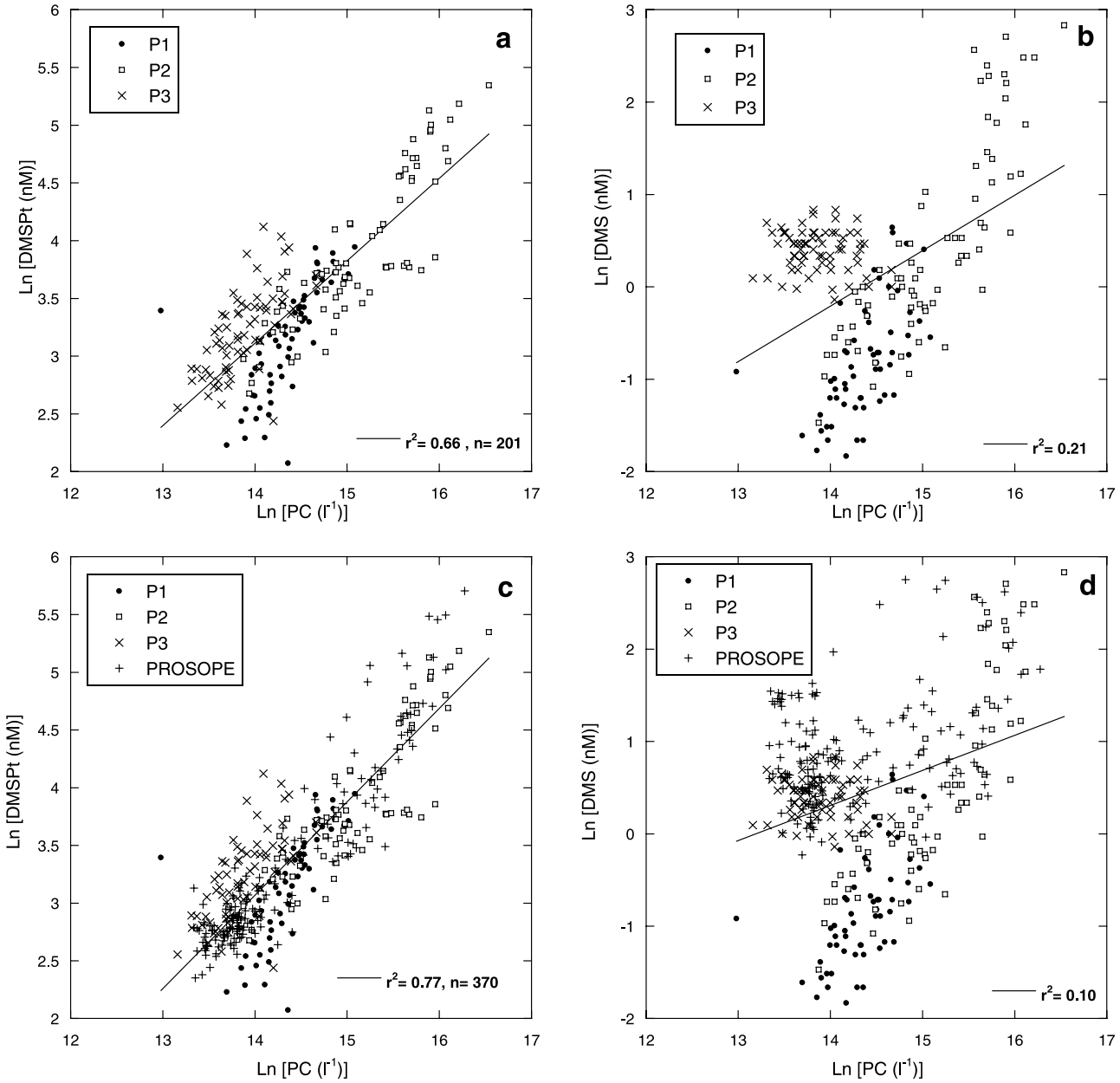

Figure 5. Scatter diagram of DMSPt and DMS sea surface concentrations plotted against total number of suspended particles from a HIAC profiler in log-transformed data. This plot is for (a, b) the POMME area and (c, d) for a broader area in the northeastern Atlantic Ocean (including a transect from Cap Ghir (Morocco) to Gibraltar) and in the Mediterranean Sea (transect from Gibraltar to the Ionian Sea carried out during cruise PROSOPE [*Belviso et al.*, 2003]).

regression line plotted in black takes the whole data set into account, including seasonal variations as in VS07. The overall relationship between DMS and the solar radiation dose (P1+P2+P3, Table 3) is significant ($P < 0.01$ because $n = 232$), but, as the value of r^2 suggests, SRD accounts for only 19% of the variance associated with DMS concentrations (Table 3). The dispersion is high (estimate error = 2.19, Table 3). The exclusion of the data points displaying DMS concentrations over 10 nM (Figure 6, $n = 6$), as recommended by VS07, does not improve the DMS versus SRD regression line ($r^2 = 0.15$, estimate error = 1.38). Moreover, regression statistics could not be improved using different SRDs obtained from the series of sensitivity tests, as described previously, since r^2 ranged between 19% and 24% (Table 3).

[28] Taken individually, the 3 data sets display contrasting results in terms of slopes, intercepts and correlation coefficients (Table 3). The relationship between DMS and SRD during P3 is not significant ($P < 0.74$), the slope is not significantly different from zero, and there is poor sensitivity

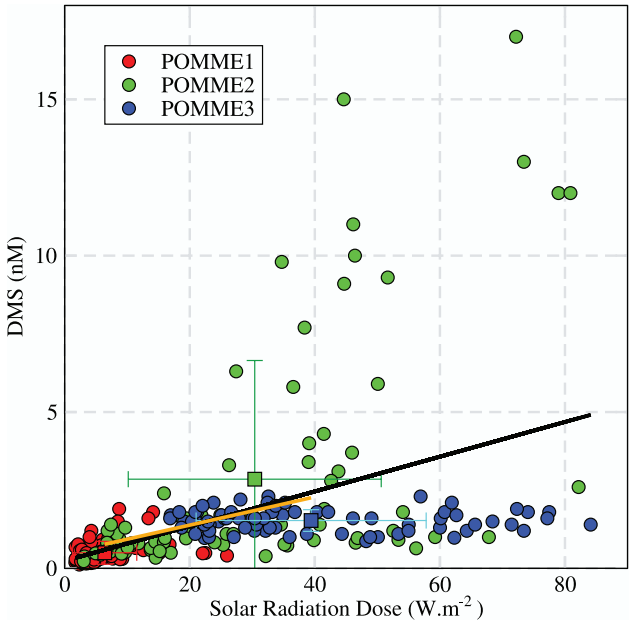

Figure 6. Linear regression (plotted in black) between DMS concentrations (in nM) and SRDs (in W/m^2) from 232 data points in total (POMME1: 78 data points; POMME2: 80 data points; POMME3: 74 data points). Superimposed are the mean and one standard deviation for each of the three cruises, together with the corresponding regression line plotted in orange (n = 3).

to the calculation method of SRDs (Table 3). For P1 and P2, results indicate that the individual linear regressions are significant because of the large number of data points taken in account (P < 0.01, Table 3), but the SRD accounts for only 9% and 30% of the variance associated with DMS concentrations, respectively. The slopes and intercepts are markedly different, and they display high sensitivity to the choice of the irradiance attenuation law. The largest dispersion is observed during cruise P2 (estimate error = 3.15, Table 3). The strongest correlations were observed during P2 (r varying between 0.51 and 0.65), but error estimates remain high between 2.85 and 3.24. Finally, it is worth noting that once an SRD formula is adopted, the series of linear regressions obtained by varying MLDs and ISIs exhibit small variations in terms of slopes and intercepts for P1 and P2. This means that the relationship between DMS and SRD heavily relies on the law of solar irradiance attenuation.

4. Discussion

[29] The POMME data sets provide a new opportunity to evaluate the relevance of the relationship put forward by VS07 between DMS and the solar radiation dose. Indeed, this new data set was acquired in the Atlantic Ocean at roughly similar temperate latitudes as Hydrostation S in the Sargasso Sea [*Dacey et al.*, 1998], although SRDs at Hydrostation S were up to 230 W/m^2 whereas a maximum of 190 W/m^2 was recorded in the POMME area (using criterion "L" (Table 2) as in VS07). Moreover, the POMME study investigated the seasonal variations of DMS and SRD, but not over several years as at Hydrostation S. The POMME data set is unique in a certain sense since, as far as we know, no other seasonal times series in Atlantic open waters exist. The fact that the survey in the Bay of Blanes may be less adequate than that for the Sargasso Sea to assess the sensitivity of DMS to changes in SRD (because of concomitant changes in algal communities in the Bay of Blanes), strengthens the importance of looking at the POMME data sets. Since we closely looked for evidences, from the POMME and other biogeochemical data sets, that variations in DMS were driven overall by changes in the abundance of total DMSP or biogenic suspended material, but found no clear indication for that (Figures 1d, 4, and 5), this would prove that the POMME area is adequate to reassess the relationship between DMS and SRD. However, we, as well as VS07, cannot exclude the possibility that the enhancement in DMS in oligotrophic surface waters could be associated with a low concentration of microorganisms that exhibit high DMSP-lyase activity.

[30] VS07 reported monthly data during the period January 1992 to November 1994, with error bars representing standard deviations of multiple sampling days each month. Therefore we calculated slopes and intercepts first from the mean SRD and DMS values obtained for each of the 3 cruises (n = 3, but each month, n = 74–80 data points), using either case "L" (0.018 nM/W m^{-2} and 0.44 nM, respectively), or case "B" (0.045 nM/W m^{-2} and 0.48 nM, respectively, Figure 6). We note that in the POMME area the slope and intercept for case "L" are almost similar to those calculated by VS07 at Hydrostation S. However, because n = 3, the

Table 3. Statistics of the Linear Regressions of DMS Concentrations Versus the SRD During POMME Cruises[a]

	Slope	Intercept	Correlation	r^2	Estimate Error	Spearman Coef.
P1 *ref.*	0.020	0.381	0.30 (p < 0.01)	0.09	0.35	0.38 (p < 0.01)
P1 *sen.*	0.007–0.051	0.252–0.381	0.30–0.41 (p < 0.01)	0.09–0.17	0.33–0.35	0.37–0.52 (p < 0.01)
P2 *ref.*	0.105	−0.167	0.55 (p < 0.01)	0.30	3.15	0.64 (p < 0.01)
P2 *sen.*	0.040–0.141	−0.734–−0.166	0.51–0.65 (p < 0.01)	0.26–0.43	2.85–3.24	0.62–0.66 (p < 0.01)
P3 *ref.*	−0.001	1.558	−0.04 (p < 0.74)	0.00	0.34	−0.02 (p < 0.84)
P3 *sen.*	−0.001–0.000	1.554–1.584	−0.06–−0.03 (p < 0.78)	0.00	0.34	−0.05–−0.02 (p < 0.84)
P1+P2+P3 *ref.*	0.051	0.392	0.44 (p < 0.01)	0.19	2.19	0.74 (p < 0.01)
P1+P2+P3 *sen.*	0.020–0.064	0.141–0.408	0.43–0.49 (p < 0.01)	0.19–0.24	2.12–2.20	0.73–0.76 (p < 0.01)

[a]*Ref* was obtained with SRD computed from SRD2, criterion "D" for the MLD and ship ISI data for P1 and P3, and ISI satellite data for P3 and P1+P2+P3. *Sen* was obtained by using the 12 sensitivity tests for the calculus of SRD (see Table 2).

correlation between SRD and DMS in the POMME area is not statistically significant either for the Pearson (for which $r = 0.66$, P < = 1) or for the Spearman rank correlation coefficient (for which $r = 0.50$, $P < = 1$).

[31] We now apply our correlation analysis to the entire POMME data set ($n = 232$) which takes into account the temporal and spatial variations in SRD and DMS. In contrast with the findings of VS07 at Hydrostation S, no strong correlation between SRD and DMS is found in the POMME area (Figure 6 and Table 3). Linear regression statistics for Hydrostation S reported by VS07 ($r^2 = 0.81$, $n = 33$, with a Spearman correlation coefficient of 0.89, $P < 0.01$) contrast with ours ($r^2 = 0.23$, $n = 232$, with a Spearman correlation coefficient of 0.75, $P < 0.01$). For consistency, we used in this later case similar criteria to that of VS07 (i.e., case "L" (Table 2): SRD1, MLD calculated using criterion $T°_{5m} - 0.1°C$). The slope and the intercept of the relationship were 0.023 nM/W m^{-2} and 0.14 nM, respectively, while VS07 reported 0.017 nM/W m^{-2} and 0.51 nM in Hydrostation S, respectively. According to the sensitivity tests we performed (Table 3), the slope and intercept of the relationships ranged between 0.02 and 0.06 nM/W m^{-2} and 0.14–0.41 nM, respectively. Hence, the slope and intercept of the VS07's relationship falls in the lower and upper ends of those ranges. The tests revealed how sensitive the relationship between DMS and SRD is to the choice of the irradiance attenuation law. When the SRD is computed from criteria "B" (Table 2, our reference case), the slope roughly doubles to 0.051 nM/W m^{-2} (Table 3). Such a large difference was unexpected according to the range of variations in slopes reported by VS07 (0.017 nM/W m^{-2} at Hydrostation S, 0.019 nM/W m^{-2} at the global scale, 0.028 nM/W m^{-2} at the Blanes Bay monitoring station, although in this later case the slope was minimized because the DMS levels higher than 10 nM were not taken into account).

[32] There is thus poor agreement between both assessments conducted in Atlantic surface waters. Herein we provide evidence that seasonal variations in DMS at the local or regional scales are not driven by the upper mixed layer solar radiation dose in the Atlantic Ocean, apart from Hydrostation S. Accordingly, the relevance of a relationship between DMS and SRD remains questionable. This is a new illustration of the difficulty in assessing the spatiotemporal distribution of DMS from empirical relationships, an approach for which important limitations have been already highlighted [*Belviso et al.*, 2004b]. Improved formulations should rely on a combination of physical and biological parameters, since biological processes play too important a role in the marine biogeochemical cycle of DMS to be neglected [*Sunda et al.*, 2007; *Vallina et al.*, 2008, and references therein].

5. Conclusion

[33] The first independent evaluation of the relationship between DMS and the Surface Radiation Dose put forward by *Vallina and Simó* [2007], shows that SRD does not well represent the seasonal variations of DMS in the Atlantic Ocean at temperate latitudes. Indeed, SRD accounted for only 19% to 24% of the variance in monthly surface DMS concentrations in the northeast Atlantic Ocean, despite accounting for 81% of the variance at Hydrostation S in the northwest Atlantic Ocean. Moreover, the relationship between DMS and SRD is heavily impacted by the choice of the irradiance attenuation law in the mixed layer and, to a lesser extent, by the criterion applied to CTD data to derive the depth of the mixed layer. In conclusion, we therefore suggest that empirical relationships relating DMS to SRD be applied with caution.

[34] **Acknowledgments.** We are grateful to A. Sciandra for providing the HIAC counter data. The authors wish to thank Laurent Mémery and Gilles Reverdin who were the scientific leaders of the POMME project and also the ship principal scientists Louis Prieur (POMME1 and POMME2) and Jean-Claude Gascard (POMME3). We also thank the captains and crew of the R/V *l'Atalante* (POMME1 and POMME2) and the R/V *la Thalassa* (POMME3). We are grateful to O. Aumont, I. Lefevre, and C. Valant who contributed to DMSP/DMS analyses during the POMME expeditions and to A. Tagliabue and L. Bopp for helpful comments on the manuscript. Finally, we also appreciate the comments of an anonymous referee and of R. Simó whose suggestions improved an earlier version of this paper. This work was supported by funding from Institut National des Sciences de l'Univers, CNRS, Météo-France, and IFREMER. This is LSCE contribution 3702.

References

Andreae, M. O. (1990), Ocean-atmosphere interactions in the global biogeochemical sulfur cycle, *Mar. Chem.*, *30*, 1–29, doi:10.1016/0304-4203(90)90059-L.

Archer, S. (2007), Crucial uncertainties in predicting biological control of DMS emission, *Environ. Chem.*, *4*, 404–405, doi:10.1071/EN07065.

Aumont, O., S. Belviso, and P. Monfray (2002), Dimethylsulfoniopropionate (DMSP) and dimethylsulfide (DMS) sea surface distributions simulated from a global ocean carbon model, *J. Geophys. Res.*, *107*(C4), 3029, doi:10.1029/1999JC000111.

Belviso, S., R. Morrow, and N. Mihalopoulos (2000a), An Atlantic meridional transect of surface water DMS concentrations with 10–15 km horizontal resolution and close examination of ocean circulation, *J. Geophys. Res.*, *105*(D11), 14,423–14,431, doi:10.1029/1999JD900955.

Belviso, S., U. Christaki, F. Vidussi, J.-C. Marty, M. Vila Reig, and M. Delgado (2000b), Diel variations of the DMSP-to-chlorophyll *a* ratio in northwestern Mediterranean surface waters, *J. Mar. Syst.*, *25*, 119–128, doi:10.1016/S0924-7963(00)00011-7.

Belviso, S., A. Sciandra, and C. Copin-Montégut (2003), Mesoscale features of surface water DMSP and DMS concentrations in the Atlantic Ocean off Morocco and in the Mediterranean Sea, *Deep Sea Res., Part I*, *50*(4), 543–555, doi:10.1016/S0967-0637(03)00032-3.

Belviso, S., C. Moulin, L. Bopp, and J. Stefels (2004a), Assessment of a global climatology of oceanic dimethylsulfide (DMS) concentrations based on SeaWiFS imagery (1998–2001), *Can. J. Fish. Aquat. Sci.*, *61*(5), 804–816, doi:10.1139/f04-001.

Belviso, S., L. Bopp, C. Moulin, J. C. Orr, T. R. Anderson, O. Aumont, S. Chu, S. Elliott, M. E. Maltrud, and R. Simó (2004b), Comparison of global climatological maps of sea surface dimethyl sulfide, *Global Biogeochem. Cycles*, *18*, GB3013, doi:10.1029/2003GB002193.

Brisson, A., P. Le Borgne, A. Marsouin, and T. Moreau (1994), Surface irradiances calculated from METEOSAT sensor data during SOFIA-ASTEX, *Int. J. Remote Sens.*, *15*, 197–203, doi:10.1080/01431169408954063.

Caniaux, G., A. Brut, D. Bourras, H. Giordani, A. Paci, L. Prieur, and G. Reverdin (2005a), A 1 year sea surface heat budget in the northeastern Atlantic basin during the POMME experiment: 1. Flux estimates, *J. Geophys. Res.*, *110*, C07S02, doi:10.1029/2004JC002596.

Caniaux, G., S. Belamari, H. Giordani, A. Paci, L. Prieur, and G. Reverdin (2005b), A 1 year sea surface heat budget in the northeastern Atlantic basin during the POMME experiment: 2. Flux correction, *J. Geophys. Res.*, *110*, C07S03, doi:10.1029/2004JC002695.

Dacey, J. W. H., F. A. Howse, A. F. Michaels, and S. G. Wakeham (1998), Temporal variability of dimethylsulfide and dimethylsulfoniopropionate in the Sargasso Sea, *Deep Sea Res., Part I*, *45*, 2085–2104, doi:10.1016/S0967-0637(98)00048-X.

de Boyer Montégut, C., G. Madec, A. S. Fischer, A. Lazar, and D. Iudicone (2004), Mixed layer depth over the global ocean: An examination of

profile data and a profile-based climatology, *J. Geophys. Res.*, *109*, C12003, doi:10.1029/2004JC002378.

Giordani, H., G. Caniaux, L. Prieur, A. Paci, and S. Giraud (2005), A one year mesoscale simulation of the northeast Atlantic: Mixed layer heat and mass budgets during the POMME experiment, *J. Geophys. Res.*, *110*, C07S08, doi:10.1029/2004JC002765.

Jerlov, N. G. (1977), Classification of sea water in terms of quanta irradiance, *J. Cons. Cons. Int. Explor. Mer.*, *37*(3), 281–287.

Kara, A. B., P. A. Rochford, and H. E. Hurlburt (2000), An optimal definition for ocean mixed layer depth, *J. Geophys. Res.*, *105*(C7), 16,803–16,821, doi:10.1029/2000JC900072.

Le Cann, B., M. Assenbaum, J.-C. Gascard, and G. Reverdin (2005), Observed mean and mesoscale upper ocean circulation in the midlatitude northeast Atlantic, *J. Geophys. Res.*, *110*, C07S05, doi:10.1029/2004JC002768.

Mémery, L., G. Reverdin, J. Paillet, and A. Oschlies (2005), Introduction to the POMME special section: Thermohaline ventilation and biogeochemical tracer distribution in the northeast Atlantic Ocean and impact of mesoscale dynamics, *J. Geophys. Res.*, *110*, C07S01, doi:10.1029/2005JC002976.

Paci, A., G. Caniaux, M. Gavart, H. Giordani, M. Lévy, L. Prieur, and G. Reverdin (2005), A high-resolution simulation of the ocean during the POMME experiment: Simulation results and comparison with observations, *J. Geophys. Res.*, *110*, C07S09, doi:10.1029/2004JC002712.

Paci, A., G. Caniaux, H. Giordani, M. Lévy, L. Prieur, and G. Reverdin (2007), A high-resolution simulation of the ocean during the POMME experiment: Mesoscale variability and near surface processes, *J. Geophys. Res.*, *112*, C04007, doi:10.1029/2005JC003389.

Paulson, C. A., and J. J. Simpson (1977), Irradiance measurements in the upper ocean, *J. Phys. Oceanogr.*, *7*, 952–956, doi:10.1175/1520-0485(1977)007<0952:IMITUO>2.0.CO;2.

Paulson, C. A., and J. J. Simpson (1981), The temperature difference across the cool skin of the ocean, *J. Geophys. Res.*, *86*(C11), 11,044–11,054, doi:10.1029/JC086iC11p11044.

Simpson, J. J., and T. D. Dickey (1981), Alternative parameterizations of downward irradiance and their dynamical significance, *J. Phys. Oceanogr.*, *11*, 876–882, doi:10.1175/1520-0485(1981)011<0876:APODIA>2.0.CO;2.

Steinke, M., G. Malin, S. D. Archer, P. H. Burkill, and P. S. Liss (2002), DMS production in a coccolithophorid bloom: Evidence for the importance of dinoflagellate DMSP lyases, *Aquat. Microb. Ecol.*, *26*, 259–270, doi:10.3354/ame026259.

Sunda, W. G., R. Hardison, R. P. Kiene, E. Bucciarelli, and H. Harada (2007), The effect of nitrogen limitation on cellular DMSP and DMS release in marine phytoplankton: Climate feedback implications, *Aquat. Sci.*, *69*, 341–351, doi:10.1007/s00027-007-0887-0.

Taylor, K. E. (2001), Summarizing multiple aspects of model performance in a single diagram, *J. Geophys. Res.*, *106*(D7), 7183–7192, doi:10.1029/2000JD900719.

Thomson, R. E., and I. V. Fine (2003), Estimating mixed layer depth from oceanic profile data, *J. Atmos. Oceanic Technol.*, *20*(2), 319–329, doi:10.1175/1520-0426(2003)020<0319:EMLDFO>2.0.CO;2.

Toole, D. A., and D. A. Siegel (2004), Light-driven cycling of dimethylsulfide (DMS) in the Sargasso Sea: Closing the loop, *Geophys. Res. Lett.*, *31*, L09308, doi:10.1029/2004GL019581.

Vallina, S. M., and R. Simó (2007), Strong relationship between DMS and the solar radiation dose over the global surface ocean, *Science*, *315*, 506–508, doi:10.1126/science.1133680.

Vallina, S. M., R. Simó, T. R. Anderson, A. Gabric, R. Cropp, and J. M. Pacheco (2008), A dynamic model of oceanic sulfur (DMOS) applied to the Sargasso Sea: Simulating the dimethylsulfide (DMS) summer paradox, *J. Geophys. Res.*, *113*, G01009, doi:10.1029/2007JG000415.

Vila, M., and M. Masó (2005), Phytoplankton functional groups and harmful algal species in anthropogenically impacted waters of the NW Mediterranean Sea, *Sci. Mar.*, *69*(1), 31–45, doi:10.3989/scimar.2005.69n131.

Vila-Costa, M., R. P. Kiene, and R. Simó (2008), Seasonal variability of the dynamics of dimethylated sulfur compounds in a coastal northwest Mediterranean site, *Limnol. Oceanogr.*, *53*(1), 198–211.

S. Belviso, Laboratoire des Sciences du Climat et de l'environnement, UMR1572, IPSL, CEA, UVSQ, CNRS, CEN de Saclay L'Orme des Merisiers, Bât 712, F-91191 Gif-sur-Yvette CEDEX, France. (sauveur.belviso@lsce.ipsl.fr)

G. Caniaux, CNRM, GAME, Météo France, CNRS, 42 Avenue G. Coriolis, F-31057 Toulouse CEDEX, France. (guy.caniaux@meteo.fr)